ADVANCED BIOLOGY
www.advanced-bio.com

Artificial Receptor in Synthetic Cells Performs Transmembrane Activation of Proteolysis

*Ane Bretschneider Søgaard, Kaja Borup Løvschall, Mireia Casanovas Montasell, Clara Bakkegaard Cramer, Pere Monge Marcet, Andreas Bøtker Pedersen, Josefine Hammer Jakobsen, and Alexander N. Zelikin**

The design of artificial, synthetic cells is a fundamentally important and fast-developing field of science. Of the diverse attributes of cellular life, artificial transmembrane signaling across the biomolecular barriers remains a high challenge with only a few documented successes. Herein, the study achieves signaling across lipid bilayers and connects an exofacial enzymatic receptor activation to an intracellular biochemical catalytic response using an artificial receptor. The mechanism of signal transduction for the artificial receptor relies on the triggered decomposition of a self-immolative linker. Receptor activation ensues its head-to-tail decomposition and the release of a secondary messenger molecule into the internal volume of the synthetic cell. Transmembrane signaling is demonstrated in synthetic cells based on liposomes and mammalian cell-sized giant unilamellar vesicles and illustrates receptor performance in cell mimics with a diverse size and composition of the lipid bilayer. In giant unilamellar vesicles, transmembrane signaling connects exofacial receptor activation with intracellular activation of proteolysis. Taken together, the results of this study take a step toward engineering receptor-mediated, responsive behavior in synthetic cells.

1. Introduction

Artificial, synthetic cells (syncells) are fundamentally intriguing and hold the potential for diverse applications in biotechnology and biomedicine.[1] Cellularity has been proven by evolution to be the foundational attribute of living organisms and as such, all life forms on Earth are cellular. Recreating life and the prospect of the *de novo* engineering of cells are among the most recognized challenges of science. Techniques to tackle this include bottom-up assembly[1b] or a top-down re-engineering of a cell.[2] The latter approach is currently much more successful, as illustrated by the recent engineering of a bacterial cell with a minimalistic genome.[1a]

The bottom-up methodologies toward the design of syncells are in many ways similar to the problem of the Origin of Life. Engineering of a fully functional, self-reproducing cell using these methods is currently well beyond reach,[1d] but certain aspects of cellular life have been successfully realized in synthetic or pre-biotic systems.[1b–d] These include the synthesis of macromolecules in primordial conditions[3] and the assembly of cell-like compartments via *de novo* synthesis of lipids.[4] Artificial host compartments for synthetic cells have been designed using diverse building blocks, of natural and/or synthetic origin.[5] Sub-compartmentalization efforts have delivered syncells with one, few, or a myriad of sub-compartments within a single syncell.[6] Another area that has been explored rather well is the encapsulated catalysis. Excellent examples have been reported for reconstitution of natural enzymatic catalysis in the volume of a syncell, including examples of multi-enzymatic systems whereby the individual enzymes are coexisting, are interconnected, and/or assembled into a cascade.[6a,7] The cell-free transcription and/or translation systems in the voids of syncells has become a mainstream tool of biotechnology.[1e] It is worth noting that as it stands, the field does not distinguish between chimeric (of natural, re-purposed building blocks) and artificial cells[1e] and in fact it is rather common that a syncell has both, natural and fully synthetic components.[1b–d] In some powerful examples, artificial cells harbor natural mitochondria,[8] nuclei,[9] or even intact bacterial cells.[10]

What seems to remain a considerable challenge is to design syncells with responsive behavior, whereby catalysis (proteolysis,

A. B. Søgaard, A. N. Zelikin
iNano Interdisciplinary Nanoscience Center
Aarhus University
Aarhus 8000, Denmark
E-mail: zelikin@chem.au.dk
K. B. Løvschall, M. C. Montasell, C. B. Cramer, P. M. Marcet, A. B. Pedersen, J. H. Jakobsen, A. N. Zelikin
Department of Chemistry
Aarhus University
Aarhus 8000, Denmark
The ORCID identification number(s) for the author(s) of this article can be found under https://doi.org/10.1002/adbi.202400053

DOI: 10.1002/adbi.202400053

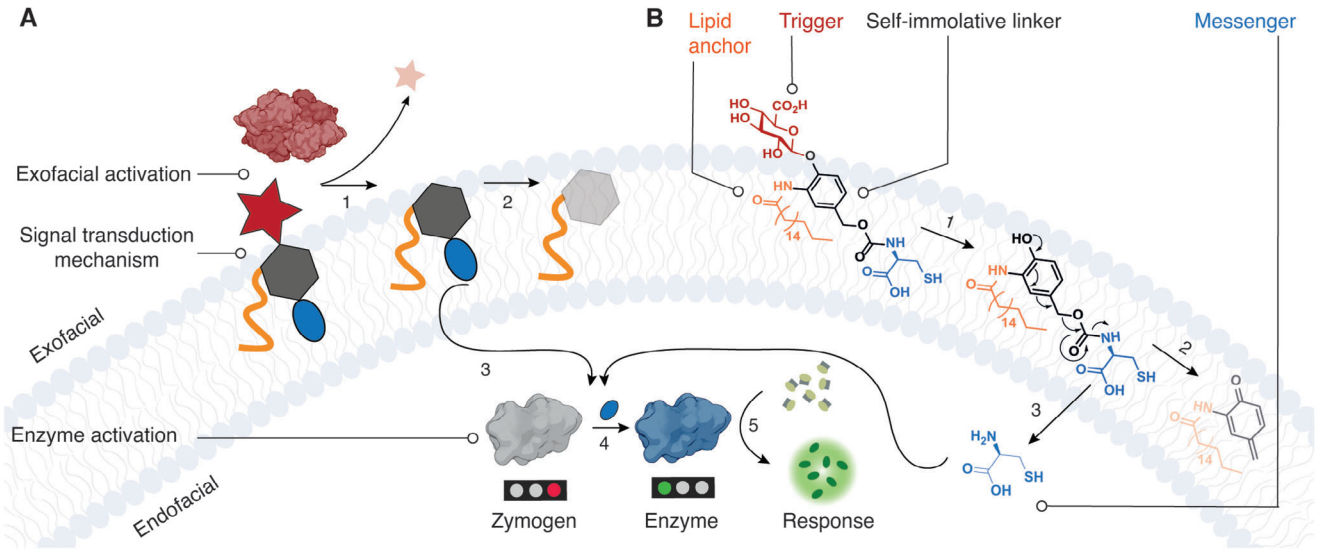

Figure 1. A) Schematic illustration and B) the chemical reactions that form the basis of the signal transduction mechanism developed in this work. The pathway consists of 1) receptor activation, 2) signal transduction via self-immolative decomposition of the receptor molecule, 3) release of the secondary messenger molecule to the interior of the syncell, 4) activation of the chemical zymogen into the corresponding active enzyme, and 5) the enzymatic output. This figure is provided for illustrative purposes and molecules are not drawn to scale.

transcription, translation, etc.) is performed in response to an external stimulus and leads to an internal adaptation of the syncell.[11] One important step toward realizing this responsive behavior in syncells is the engineering of their communicative behavior. By far, most examples in the field approach communication using soluble, diffusible molecules, and exploit syncells with (semi)permeable compartment boundaries.[7b,12] For example, coacervate-based syncells have been engineered to respond to infiltrating proteins and nucleic acids.[13] In the examples where a syncell is defined by a lipid bilayer, communication has been accomplished using bilayer-permeable molecules[12,14] or transporter proteins embedded in the lipid bilayer.[7b] These examples are highly important in their own right. Nevertheless, the most important mechanism of communication designed by Nature, namely communication using transmembrane receptors, remains the most challenging to engineer in the context of syncells.

Transmembrane signaling using the tools of organic chemistry has had few successes. First example is based on the principle of chemically induced dimerization, mimicking the mechanism of transmembrane signaling by the natural receptor tyrosine kinases. Here, exofacially induced dimerization of membrane-spanning organic molecules ensues the dimerization of the intracellular tails of the molecules, which can lead to a chemical reaction or a change in the fluorescence quantum yield.[15] The second well-documented mechanism of transmembrane signaling relies on the triggered "bobber-like" behavior of a bilayer-anchored molecule. Here, an exofacial binding event enables an immersion of the bobber-molecule into the lipid bilayer causing exposure of its tail in the internal of the syncell. Prominent examples of this design include transmembrane signaling in response to a change in pH,[16] the binding of metal ions,[17] expose to light,[18] and a redox reaction[19] at the surface of a syncell (liposome). In other examples, bobber-like behavior of the membrane-bound molecules was mediated by light[20] or host-guest interactions.[21] The above systems are inspirational but their utility in the design of syncells (beyond transmembrane signaling) is yet to be disclosed. A recent important step toward transmembrane signaling that culminates in a relevant biochemical response[22] involved dynamic covalent chemistry to facilitate the translocation of an enzyme-activating molecule.

In our own recent work, we recognized that the design of syncells with responsive behavior is a two-part problem, and it requires the development of i) transmembrane signaling and ii) downstream signaling pathways (**Figure 1A**).[14,23] Moreover, the two stages have to operate on the same chemical platform, to be coupled into an overall receptor-mediated responsive behavior. As a chemical platform, we chose the chemistry of thiols. "Thiol switching" is a natural mechanism to control the activity of enzymes,[24] although hardly used in Nature in the design of signaling cascades. In our hands, the reversible thiol-to-disulfide conversion proved to be an efficient on/off switch for activity of cysteine proteases, such as papain, creatine kinase and the T7 polymerase.[14,25] We used these enzyme activity-switching events to establish downstream signaling pathways in syncells.[14]

For transmembrane signal transduction, we designed an artificial receptor that releases a thiol-containing secondary messenger molecule (Figure 1B).[23] Using the toolbox of prodrug design,[26] we applied the chemistry of self-immolative linkers (SILs) as a mechanism for signal transduction. Exofacial receptor activation was performed by an enzyme, to trigger the decomposition of the SIL (via *1,6*-benzyl elimination) and afforded the release of L-cysteine (L-Cys). This natural thiol-containing amino acid was released into the lumen of the liposomal syncell, wherein it activated a disulfide-protected cysteine protease, to restore its activity.[23] Thus, an exofacial enzymatic receptor activation event was communicated by a chemical receptor across the lipid bilayer and afforded intracellular activation of an enzyme.

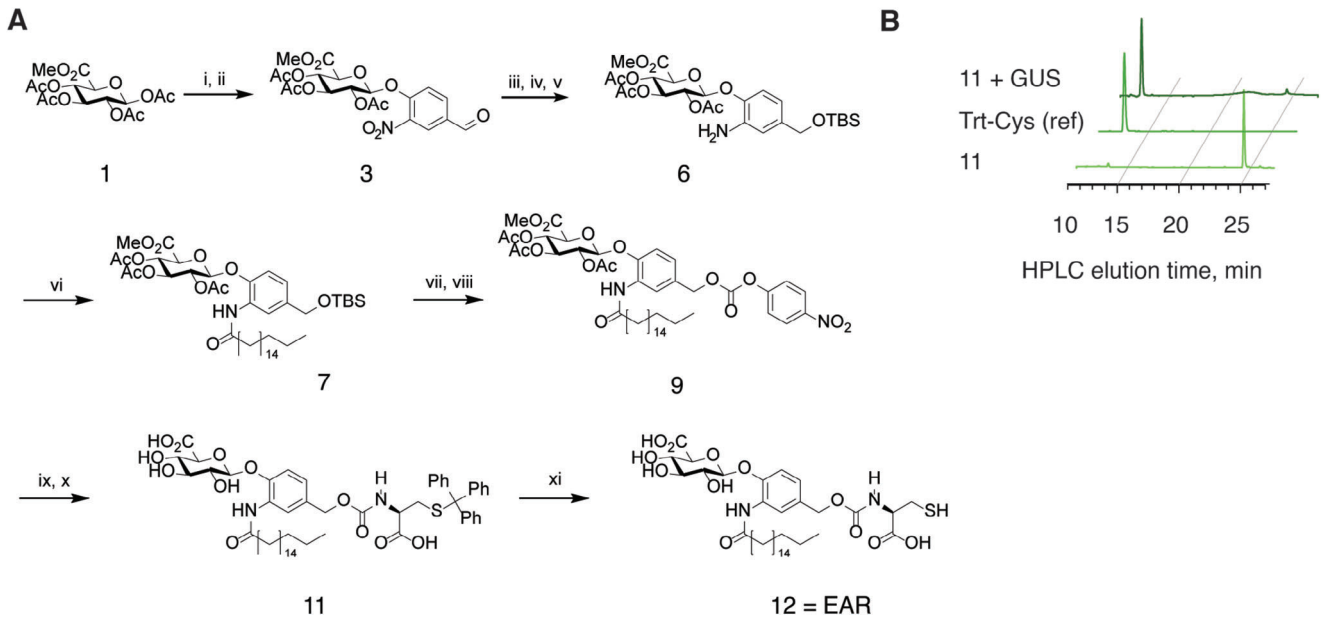

Figure 2. The synthesis and characterization of the glucuronidase-specific enzyme activating receptor (Gus-EAR) A) Schematic illustration of the synthesis of the artificial signaling receptor Gus-EAR via an 11-step linear synthesis; B) characterization of the enzyme-mediated decomposition of the compound 11 via HPLC. For details of the synthesis, please see Experimental Section.

In this work, we focus on the transmembrane signaling and develop this event from the proof-of-concept into an in-detail characterized platform. Specifically, we 1) re-design and scale up the artificial receptor synthesis, 2) demonstrate the specificity of receptor cross-activation by non-cognate enzymes, 3) validate signaling across bilayers varied by lipid composition and by size, and as a dose-responsive event for the activating enzyme, 4) engineer transmembrane signaling into cell-sized GUVs, and 5) demonstrate signaling that culminates in an encapsulated proteolysis, mimicking Nature. These results take a step toward realizing receptor-mediated responsive behavior in syncells and increase the life-likeliness of artificial cell mimics.

2. Results and Discussion

The first step in this study considered the re-design of the synthesis path to the artificial signaling receptor. In our previous study,[23] we observed that the β-glucuronidase-specific **e**nzyme **a**ctivating **r**eceptor (Gus-EAR, Figure 1B) was attractive as a candidate for broader implementations in the design of syncells, but the synthesis was troublesome, specifically as regards to the reaction yields. Herein, Gus-EAR was synthesized via an 11-step synthesis, starting with methyl 1,2,3,4-tetra-O-acetyl-β-D-glucuronate, (compound **1**, **Figure** 2A). 4-hydroxy-3-nitrobenzaldehyde formed the template of the SIL scaffold, chemical *O*-glycosylation delivered the required beta-diastereomer for enzyme recognition in molecule **3**. Reduction of the aldehyde and nitro- moieties delivered the chemical handles in molecule **6**, for the secondary messenger and the lipid bilayer anchor, respectively. For bilayer anchoring of the receptor molecule, we used stearic acid, a naturally occurring fatty acid. The acyl chloride of steric acid reacted smoothly with the amine on compound **6** in the presence of triethylamine to deliver the desired amide in **7**. Although the newly developed synthesis is linear rather than the previously used convergent path,[23] the total yield from **1** to **7** was enhanced from under 4% to over 30%. Next, *S*-Trityl-L-cysteine was introduced via a carbonate exchange reaction with mixed carbonate **9** to afford **10** in 80% yield. Finally, deprotection of glucuronic acid afforded the *S*-trityl protected Gus-EAR molecule, **11**. Compound **11** was used in the HPLC characterization of receptor activation and release of the secondary messenger, taking advantage of the ease of detection of the trityl-group. Compound **11** was stable in solution and revealed no signs of spontaneous decomposition. Upon addition of the β-glucuronidase (GUS) enzyme, **11** quantitatively released *S*-trityl-L-cysteine (Figure 2B), illustrating enzyme activated release of the (*S*-trityl-protected) secondary messenger molecule, in solution. Lastly, removal of the trityl-group using triflouroacetic acid and triisopropylsilane on compound **11** afforded the desired Gus-EAR molecule, **12**.

To illustrate the principle of transmembrane signaling, we used liposomes as the simplest mimics of a natural cell. Liposomes were assembled using egg yolk α-L-phosphatidylcholine (EPC) via the rehydration of a thin lipid film. The rehydration buffer contained the disulfide-based zymogen of the papain protease and a fluorogenic substrate for papain, N_α-benzoyl-L-arginine-7-amido-4-methylcoumarin (Arg-AMC). Thiol-disulfide exchange between the protein and the releasable secondary messenger, L-Cys, is poised to liberate the protein active site thiol and in doing so, to restore the enzymatic activity of the enzyme, which would be reported by the increase in solution fluorescence.[22–23,25a,27] To validate the syncell system, we first performed transmembrane activation of the papain zymogen using a bilayer-permeable reducing agent, dithiothreitol (DTT). Addition of DTT to the liposomal zymogen expectedly afforded a strong fluorescent signal, indicative of the zymogen reactivation (**Figure** 3A,B). The aminoacid cysteine is a zwitterion and is

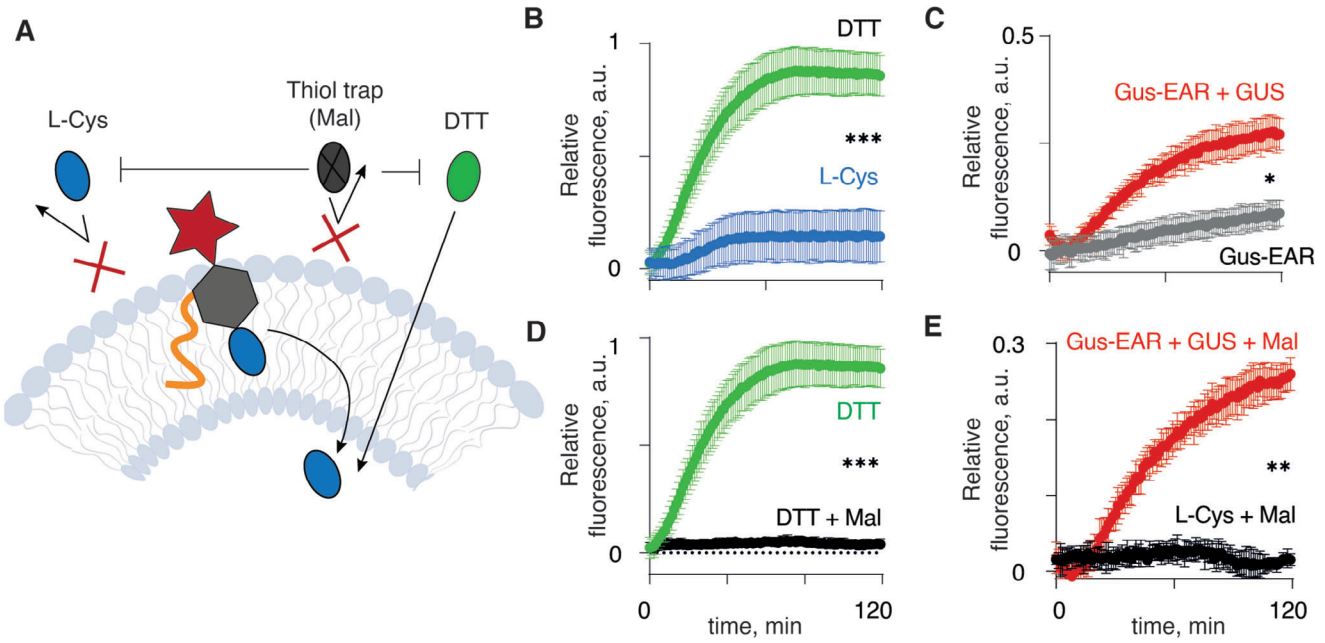

Figure 3. Transmembrane signaling in a liposomal syncell. A) Schematic illustration of transmembrane activation of the liposome-encapsulated zymogen for papain, by DTT or L-Cys via the diffusive mechanism, or by the enzyme-activated receptor via transmembrane signaling; B–E) experimental data illustrating transmembrane activation of the papain zymogen by 10 μM DTT or 20 μM L-Cys (B), C) by 20 μM Gus-EAR with and without the addition of the activating GUS enzyme, D) by DTT in the presence or absence of the thiol trap maleimide-$PEG_{5000\ Da}$, and E) by Gus-EAR upon enzyme activation or by externally added L-Cys, in the presence of the thiol trap. Mal = maleimide-$PEG_{5000\ Da}$. In panels B-E: presented results are based on three independent experiments and shown as mean ± st. dev. Statistical evaluation was performed using the end-point fluorescence intensity values via one-way ANOVA, $^{*}p < 0.05$, $^{**}p < 0.01$, $^{***}p < 0.001$.

expected to have significantly restricted permeability across a lipid bilayer. Indeed, relative to DTT and at matched thiol concentrations, L-Cys exhibited a limited efficacy of activation of the liposomal zymogen for papain (Figure 3A,B). Liposomes that received only Gus-EAR (no external enzyme activator) exhibited only minor evolution of fluorescence, which indicates that the receptor thiol group does not have access to the disulfide linkage of the zymogen in the liposome lumen (Figure 3C). In other words, the receptor molecules do not translocate across the lipid bilayer into the inner volume of the liposome. The addition of GUS to this solution afforded a significant increase in fluorescence, indicating that Gus-EAR undergoes activation and releases the secondary messenger, which then navigates into the inner volume of the liposomes and activates the encapsulated papain zymogen (Figure 3C). It is worth noting that the zymogen reactivation within the syncells occurs via thiol-disulfide exchange, which is a dynamic equilibrium process. The papain cysteine thiol has an unusually low pKa,[28] which makes it a better-leaving group compared to the blocking group L-cysteine, and the release of the papain thiol from a mixed disulfide is therefore thermodynamically favorable.

Activation of the liposomal papain zymogen was also performed in the presence of a thiol trap, a maleimide derivative of 5 kDa polyethylene glycol (PEG), added externally to the suspension of liposomes (Figure 3D,E). Under these conditions, activation of papain zymogen by DTT was inhibited in full (Figure 3D). Zymogen activation by L-Cys was also negligible (Figure 3E). In stark contrast, the thiol trap had little if any effect on the reactivation of the liposomal zymogen using the enzyme-activated Gus-EAR (Figure 3E). Qualitatively and quantitatively, these data are very similar to the transmembrane signaling that we have previously disclosed for an EAR molecule that is specific to the external activity of alkaline phosphatase (ALP).[23]

The experiments in Figure 3 indicate that the externally added thiol trap has no access to the papain thiol (c.f. Figure 3E) and the inhibitory activity of this maleimide on the zymogen reactivation is due to the reaction between the maleimide and the thiols in the external solution bulk. These results further illustrate that the thiol in the structure of Gus-EAR is not accessible to the maleimide (Figure 3E) strongly suggesting that the thiol is localized within the lipid bilayer. Most importantly, the data indicate that the secondary messenger released from Gus-EAR upon receptor activation also escapes the thiol scavenger, meaning that the observed zymogen reactivation is due to the thiols that are released by the receptor molecule directly into the lumen of the liposome. Taken together, this implies that activation of the encapsulated papain zymogen by the Gus-EAR upon external addition of GUS is a transmembrane signaling event. This mechanism enables activation of the encapsulated papain zymogen in conditions where activity of the soluble activators (DTT, L-Cys) is arrested.

To illustrate selectivity and specificity of the receptor-mediated transmembrane signaling in liposomes, we used Gus-EAR molecules cognate to the GUS enzyme and attempted to perform receptor activation using three diverse enzymes: GUS, β-glucosidase (GLU), and ALP (**Figure** 4A). In these experiments, we observed no activation of the papain zymogen

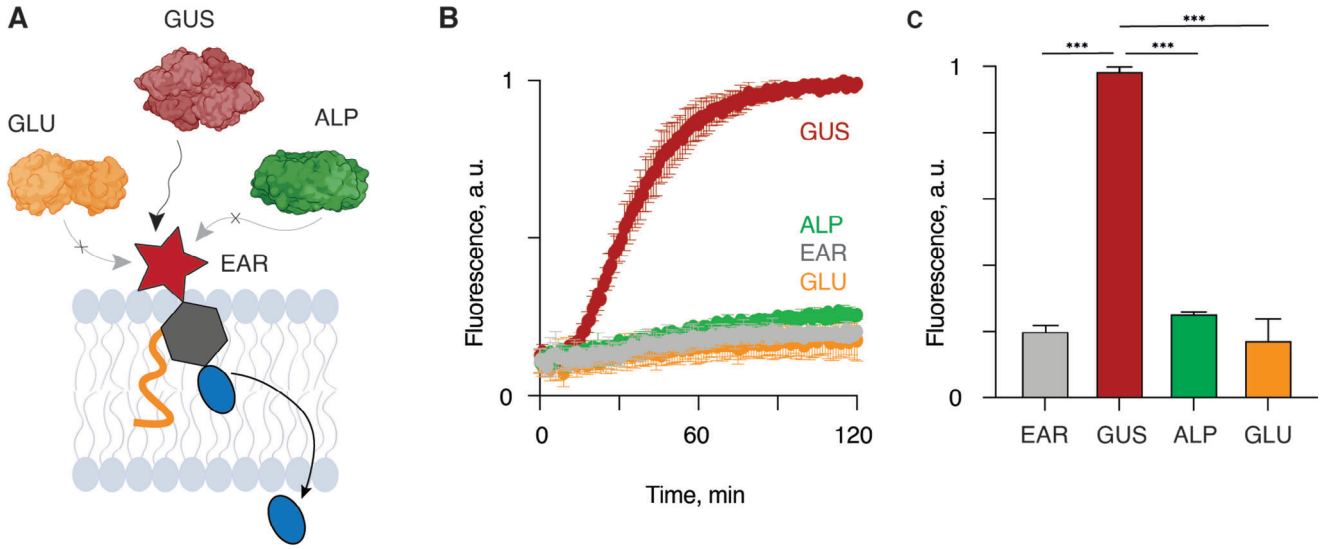

Figure 4. Selectivity in the enzyme activation of the artificial receptor. A) Schematic illustration and B,C) experimental data illustrating activation of the Gus-EAR using β-glucuronidase (GUS), β-glucosidase (GLU), or alkaline phosphatase (ALP). Gus-EAR was installed on the liposomes, and receptor activation is reflected by the reactivation of the encapsulated papain zymogen. In panels (B, C): the presented results are based on three independent experiments and shown as mean ± st. dev. In panel (C), statistical evaluation was conducted via one-way ANOVA, $^{***}p < 0.001$.

by Gus-EAR upon external addition of ALP or GLU, and an insignificant background activation of the Gus-EAR alone (Figure 4B,C). In contrast, addition of GUS resulted in a strong development of solution fluorescence, indicative of receptor activation and ensuing activation of the liposomal encapsulated papain zymogen (Figure 4B,C). Thus, transmembrane signaling by the Gus-EAR molecules is specific, with minimal non-specific activation. Together with the use of thiol scavengers in the extracellular space, it offers the highly desired possibility of specific activation of the nominated, receptor-containing synthetic cells.

The central point in the characterization of transmembrane signaling by artificial receptors is how flexible and adaptable the system is when varying the composition of the lipid bilayer. Indeed, depending on the chemical structure, lipids exhibit varied melting temperatures; fluidity and permeability of the barrier can be further dependent on the presence of cholesterol and other membrane constituents.[20b] With the highest relevance to our study, these parameters have been previously shown to affect transmembrane signaling in syncells.[20b] Herein, we employed two lipids: EPC (melting point 13 °C) and 1-palmitoyl-2-oleoyl-glycero-3-phosphocholine (POPC, melting point – 3 °C). We also examined two levels of cholesterol content (10 and 30 wt.%), added to gain similarity with natural mammalian membranes which contain ≈20 wt.% of cholesterol.[29] In all experiments, transmembrane signaling was quantified in the presence of the thiol trap in the extracellular solution. These results are presented in **Figure** 5A relative to the zymogen activation by DTT in the absence of the thiol trap, in liposomes assembled using the corresponding lipids.

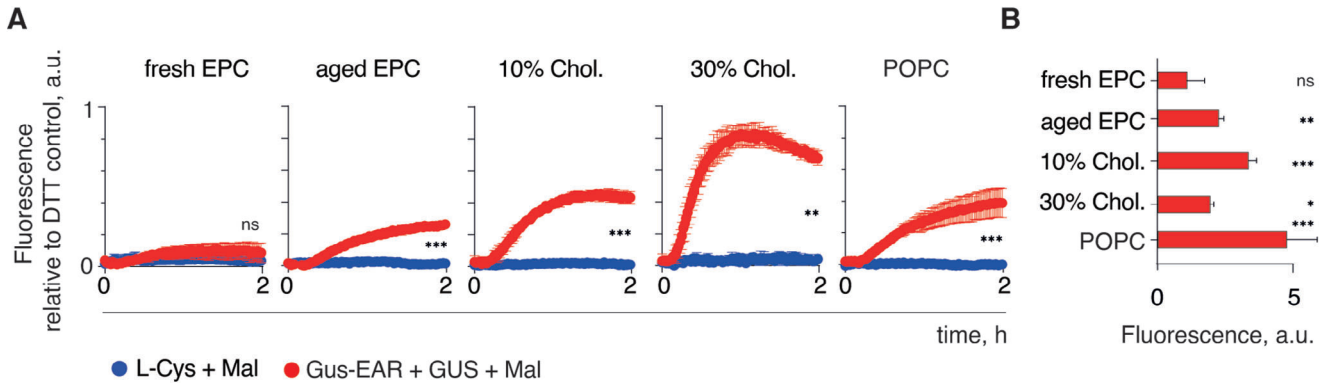

Figure 5. Transmembrane signaling as a function of lipid composition. Transmembrane signaling as a result of activation of Gus-EAR by GUS in 200 nm liposomes composed of EPC (fresh or aged) or POPC, optionally supplemented with cholesterol to 10 or 30 weight %, in the presence of the thiol trap, PEG maleimide, relative to the zymogen activation by DTT in the absence of the thiol trap in the liposomes assembled using the corresponding lipids A) and in absolute numerical values B). The presented results are based on three independent experiments and shown as mean ± st. dev.; statistical evaluation was conducted via one-way ANOVA for the end-point readings at 2 h; in panel B, statistical evaluation is reported relative to the non-activated samples; $^{***}p < 0.001$, $^{**}p < 0.01$, $^{*}p < 0.05$, ns = non-significant.

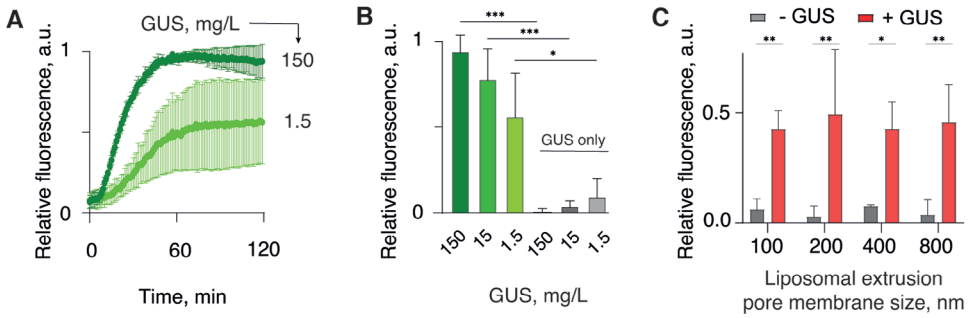

Figure 6. Dose- and size-dependent effects in transmembrane signaling. A) Transmembrane signaling by Gus-EAR as triggered by GUS at 150 or 1.5 mg L^{-1}; B,C) End-point measurement of enzymatic output by the liposomal papain as a result of transmembrane signaling by Gus-EAR activated by GUS at varied concentrations (B), and by Gus-EAR in the presence of 150 mg L^{-1} GUS in liposomes prepared via extrusion through membranes with sizes from 100 to 800 nm (C). In all panels, concentration of Gus-EAR was 20 μM; in panels A,B: transmembrane signaling was recorded in the presence of 50 μM PEG maleimide; the presented results are based on three independent experiments and shown as mean ± st. dev.; statistical evaluation was conducted via one-way ANOVA, $^{***}p < 0.001$, $^{**}p < 0.01$, $^{*}p < 0.05$, non-significant is not indicated.

During the course of our experiments, we observed that EPC undergoes "aging", and liposomes prepared from fresh lipids support minor transmembrane signaling (at 20 μM Gus-EAR), whereas "aged" EPC makes up the liposomes in which signaling is well pronounced (Figure 5A). The origin of this observation remains unclear. Using aged EPC, receptor-mediated signaling was enhanced by the presence of cholesterol in the lipid bilayer, thus being the direct opposite of the influence of cholesterol on transmembrane signaling that relies solely on diffusion.[20b] In the presence of 30 wt.% cholesterol, the activation of the encapsulated zymogen achieved via transmembrane signaling using Gus-EAR was nearly as efficacious as that achieved by DTT. Signaling in liposomes comprised of POPC was also reliable and pronounced.

The original thought of using DTT as a control in Figure 5A was that it serves as an indicator for the maximum zymogen reactivation under the specific experimental settings. However, we noticed that the numerical values that reflect zymogen reactivation by DTT varied significantly with the change in lipid composition, which likely reflects the altered diffusivity of DTT through the varied lipid bilayers (Figure S1, Supporting Information).[20b] For instance, zymogen reactivation using DTT in the EPC-based liposomes was significantly lowered by the presence of cholesterol (Figure S1, Supporting Information). At the same time, in absolute numerical values, transmembrane signaling by activated Gus-EAR was enhanced (for 10 wt.% content) or only marginally decreased (for 30 wt.% content) by the presence of cholesterol (Figure 5B). Thus, the conclusion that transmembrane signaling in the presence of 30 wt.% cholesterol being the most pronounced (Figure 5A) is to a significant extent due to the normalization of the raw data. Nevertheless, the main conclusions on the transmembrane signaling using activated Gus-EAR remain the same when viewed relative to DTT or seen using absolute numerical values that reflect zymogen reactivation (Figure 5B): transmembrane signaling by activated Gus-EAR was statistically significant in all liposomal compositions expect for the fresh EPC. These results illustrate that transmembrane signaling by Gus-EAR can be achieved in a range of compositions of the lipid bilayer, and specifically in the presence of cholesterol at or near its physiological content in the lipid bilayer. Worthy of note, regardless of lipid composition, transmembrane activation of the papain zymogen exhibited an approximately 15–25 min lag time (Figure 5A). This time being rather constant and independent of the lipid composition of the bilayer, it likely reflects the kinetics of the exofacial enzymatic catalysis and the decomposition of the SIL and is thus a characteristic signaling time for Gus-EAR.

Another important step in the characterization of transmembrane signaling mediated by Gus-EAR is to document the dose responses for both the receptor molecule and the activating enzyme. We found that the variation in the content of the activating enzyme had only a minor effect on transmembrane signaling. Indeed, a 100-fold variation in GUS enzyme concentration afforded less than a 2-fold change in transmembrane signaling (**Figure 6A,B**). As low as 1.5 mg L^{-1} of GUS was sufficient to induce statistically significant transmembrane signaling by Gus-EAR. As regards the receptor content, we observed that freshly prepared solutions of Gus-EAR afforded significant transmembrane signaling at concentrations as low as 5 μM. We believe that this is consistent with the typical Michaelis-Menten constants for GUS enzyme, which are micromolar.[30] Upon storage (as stock solutions in DMSO or NMP), Gus-EAR exhibited a gradual loss of activity through oxidation. Quite unexpectedly, we also observed that Gus-EAR undergoes chemical decomposition over time; we are now investigating the mechanism of this process and will report it in subsequent publications. Nevertheless, over numerous rounds of experiments, we observed that 20 μM receptor concentration afforded reproducible, reliable transmembrane activation of the liposomal papain zymogen (as is illustrated by the data presented throughout this manuscript).

Lastly, we also aimed to investigate if the size of the liposome is a factor that would affect signaling. We saw this as likely, because at constant total lipid content in solution, the variation in the liposome radius would lead to a change in the total number of liposomes, and thereby a change in the receptor-per-liposome content, as well as a change in the volume of each liposome, and all these factors combined would define the concentration of secondary messenger in the liposome achieved via receptor-mediated signal transduction. We performed transmembrane signaling in liposomes with sizes varied from <200 to 800 nm (liposome extrusion through membranes at 100, 200, 400, and 800 nm), Figure 6C. In all cases, the total lipid content and the

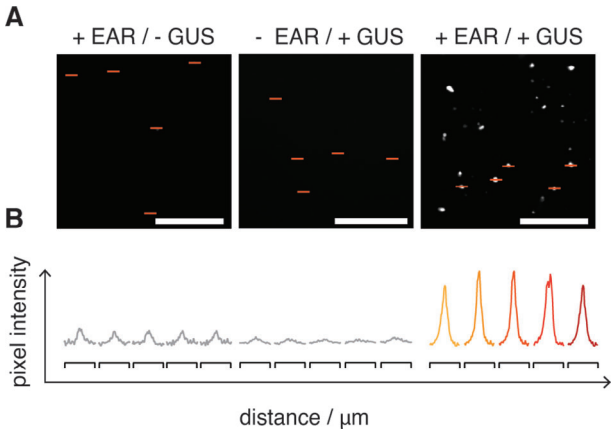

Figure 7. Fluorescence microscopy visualization of transmembrane signaling by Gus-EAR upon addition of the activating enzyme GUS in 800 nm liposomes: A) microscopy images, scale bars: 20 µm B) quantification of pixel intensity for the liposomes shown in panel A.; intensity profile traces are 4 µm each.

concentration of Gus-EAR added to the liposomes were kept constant. The most important conclusions from these experiments are that regardless of the liposome size, we observed reliable, statistically significant receptor-mediated transmembrane signaling using the enzyme-activated Gus-EAR, and no difference between the liposomal sizes ($p > 0.05$).

To visualize transmembrane signaling, we first used the largest tested, 800 nm liposomes. Zymogen-containing liposomes equipped with Gus-EAR exhibited reporter fluorescence levels only marginally above the background level, illustrating negligibly low activity of the receptor in its resting state (**Figure 7**). The addition of GUS to the receptor-negative liposomes also afforded a negligible increase in fluorescence. In stark contrast, addition of GUS enzyme to the receptor-containing liposomes led to a pronounced increase in fluorescence within liposomal compartments, viewed as sub-micrometer bright fluorescence loci (Figure 7) thus providing direct visualization of the transmembrane signaling mediated by the enzyme-activated Gus-EAR. Taken together, results presented in Figures 3–7 illustrate that transmembrane signaling mediated by the synthetic, chemical receptor is a robust methodology and signal transduction can be achieved across the bilayers with varied lipid composition, in liposomes with varied size.

As a step toward the design of synthetic cells that match their natural counterparts by size, we engineered receptor-mediated signaling into GUVs. These host compartments are the most used mimics of natural mammalian cells.[1c,d] The volume of GUVs is sufficient to encapsulate complex biochemical mixtures and even reconstitute full transcription/translation machinery.[5c] For Gus-EAR mediated signaling, we assembled GUVs via the emulsion transfer method (**Figure 8A**), using EPC as the main lipid component and 17 wt.% cholesterol. The lipid mixture also contained PEG-DSPE to enhance the GUV colloidal stability, and included rhodamine labeled phosphoethanolamine to facilitate fluorescence miscroscopy visualization (Figure 8B). The inner volume of the GUVs contained the papain zymogen and a substrate for papain, namely a preparation of albumin that had been functionalized with fluorescein to a level above the fluorescence self-quenching. GUVs were equipped with Gus-EAR and then exposed to the activating enzyme, GUS. In the absence of Gus-EAR, the addition of the enzyme resulted in minor if any development of fluorescence in the voids of GUVs in the channel corresponding to the fluorescence of fluorescein (green), that is, in minimal receptor-mediated signal transduction and papain reactivation (Figure 8B,C). Similarly, the use of Gus-EAR alone, without an addition of the receptor-activating enzyme, GUVs exhibited only minor papain reactivation. In turn, the receptor-containing GUVs, upon the addition of GUS, developed fluorescence in the confines of the GUVs. The latter results was indicative of receptor activation, ensuing signal transduction, and the activation of the papain zymogen within the syncell. Seen together, receptor mediated transmembrane signaling resulted in the activation of proteolysis within the volume of the syncells in a process that mimics extracellular activation of proteolysis in natural cells.

3. Conclusion

In this work, we assembled model synthetic cells based on liposomes and GUVs, specifically to characterize transmembrane signaling by the synthetic artificial receptor, Gus-EAR. The first accomplishment of this work was that we established a more robust synthesis of Gus-EAR via the relatively high-yield reactions, which is imperative for the product scale-up. We illustrated that the exofacial receptor activation by the cognate enzyme, GUS, is performed in a specific manner and no receptor activation is observed in the presence of non-cognate enzymes. Signal transduction was registered in liposomes with a varied lipid composition, in liposomes of varied size, and in GUVs, thus illustrating a flexible, adaptive nature of signaling. Transmembrane signaling developed in this work culminates in the release of the secondary messenger molecule, a thiol-containing amino acid L-Cys. It is readily coupled to downstream signaling cascades established around the protein cysteinome and the "thiol switching" platform for reversible enzyme activation. We believe our results form an important step toward the development of stimuli-responsive synthetic cells and enhance the life-likeliness of artificial cells assembled via the bottom-up techniques.

For broader context, we note that in our prior studies, we presented receptors of this type (that is, signal transduction via the triggered 1,6-benzyl elimination and decomposition of the artificial receptor) and their use to achieve transmembrane signaling in mammalian cells.[26b] The main difference to the Gus-EAR receptor used in this work was the choice of the suitable secondary messenger, to achieve the desired intracellular effects in response to an extracellular trigger event.[26b] Taken together, our work paves the way to chemical, non-genetic engineering of cells, both synthetic and mammalian.

4. Experimental Section

Chemistry Methods: All chemicals and solvents were acquired from Sigma–Aldrich and used without further purification unless otherwise stated. *N,N*-Dimethylformamide (DMF), trimethylamine (TEA), and methanol were obtained in anhydrous state. The solvents acetonitrile,

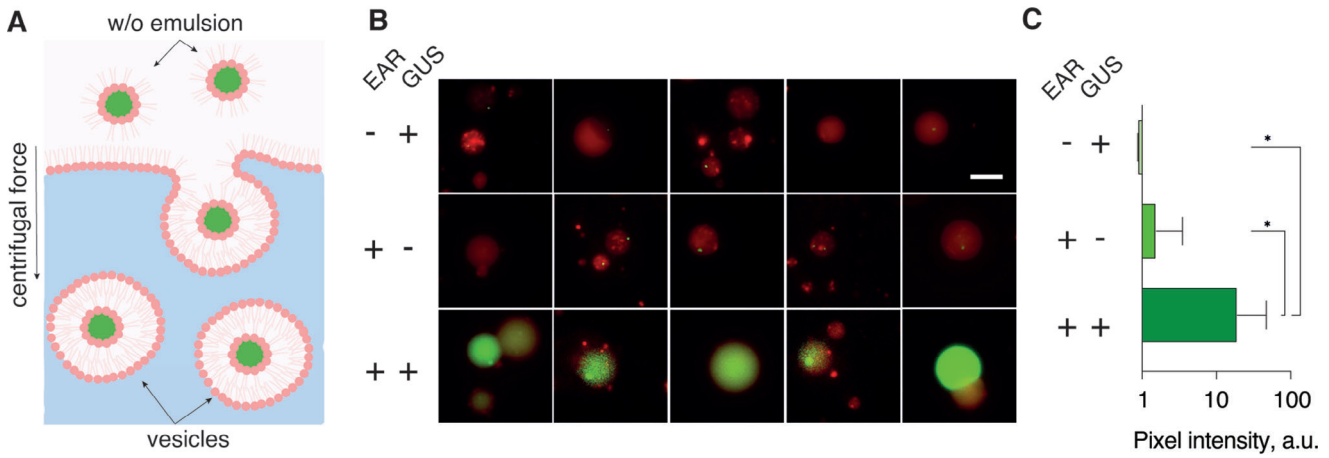

Figure 8. Visualization of transmembrane signaling by Gus-EAR in GUVs resulting in proteolytic cleavage of albumin. A) Schematic illustration of the assembly of GUVs via the emulsion transfer method; B) Fluorescence microscopy visualization of GUVs, whereby the lipid bilayer is visualized via the fluorescence of rhodamine-labeled phosphoethanolamine (shown in red), and enzymatic activity in the void of GUV is due to the proteolytic processing of the fluorogenic substrate of papain, namely albumin labeled with fluorescein over the level of self-quenching (shown in green); scale bar (same for all images): 50 µm; C) quantification of pixel intensity for the GUVs as shown in panel B; statistical evaluation is based on at least 17 GUVs and performed via one-way ANOVA, $^{*}p < 0.01$.

dichloromethane, and tetrahydrofurane (THF) were dried over aluminum oxide using a MBraun SP800 purification system. The deuterated solvents used for ^{1}H-NMR and ^{13}C-NMR analysis were purchased from Eurisotop. Thin layer chromatography (TLC) analysis was performed using silica-coated aluminum foil plates (Merck Kieselgel 60 F254) and the plates were analyzed by visualizing either by UV irradiation and/or staining with $KMnO_4$. High-purity grade silica gel (w/Ca, ≈0.1%, 230–400 mesh particle size, 60 Å pore size) was the stationary phase, which was used for silica column chromatography. A Bruker BioSpin Gmbh 400 MHz spectrometer or a Varian Mercury 400 MHz spectrometer were used for recording nuclear magnetic resonance (NMR) spectra as either ^{1}H-NMR 400 MHz or ^{13}C-NMR 101 MHz. The spectra were referenced to the residual solvent peak. High-resolution mass spectrometry (HR-MS) was performed using a Bruker Micromass LC-TOF with electrospray ionization (ESI) and analyzed with Bruker DataAnalysis. High-performance liquid chromatography (HPLC) experiments were conducted with an Agilent 1260 Infinity II connected to an EC-C18 column with particle size of 2.7 µm, length of 100 mm, and diameter of 4.6 mm. The mobile phase was a combination of ultrapure water with trifluoroacetic acid (TFA, 0.1% v/v%, eluent A) and HPLC grade acetonitrile with TFA (0.1% v/v%, eluent B). HPLC experiments were performed with the following method; started at 5% eluent B content and the eluent B content was gradually increased to 100% within 18 min and kept at 100% content for additional 13 min (total time of 31 min). UV was measured at the wavelengths $\lambda = 210$ nm and $\lambda = 254$ nm.

For compound synthesis and characterization, see Supporting Information.

General Information: Unless otherwise stated, all the chemicals are purchased from Sigma–Aldrich/Merck. The buffer used in all the following experiments is a 20 mM 4-(2-hydroxymethyl)−1-piperazineethanesulfonic acid (HEPES) buffer, adjusted to pH 6.8 and filtered through a 0.2 µm filter. This buffer will be referred to as the HEPES buffer in all the following experiments. Kinetic measurements of enzymatic catalysis were performed using a BioTek Synergy H1 microplate reader with Gen5 3.5 software. Fluorescence development of 7-amido-4-methylcoumarin (AMC) was measured at λ_{ex} 348 nm, λ_{em} 443 nm. Fluorescence microscopy was performed using a Zeiss Axio Observer Z1 equipped with a 40X and 63X lens, with a HXP 120C lamp and image analysis was performed using ImageJ version 2.9.0/1.53.

General Liposome Protocol: L-α-phosphatidylcholine from egg yolk (EPC) was dissolved at 25 g L^{-1} in chloroform and 6.25 mg EPC in chloroform (250 µL) was added to a pointy 5 mL pear-shaped flask and a thin lipid film was prepared by evaporation of chloroform using N_2. Complete evaporation and formation of the lipid film were ensured by overnight incubation in a desiccator. The film was hydrated using 100 µL HEPES buffer containing 10 g L^{-1} Papain (inactive, *REF: 26220*) and 1 mM N_{α}-benzoyl-l-arginine-7-amido-4-methylcoumarin (Arg-AMC) from *Bachem* with a final Vol% of DMSO = 1. The sample was vortexed until full rehydration (2-5 min) of the film, then additionally 150 µL HEPES buffer was added. The liposome sample was then extruded 15 times through 200 nm Whatman Nuclepore Track-Etched Membranes before the sample was purified using Size exclusion chromatography (SEC). The SEC-column was packed with degassed Sepharose CL-2B (H: 10 D: 1 cm) and calibrated with a minimum of 30 mL HEPES buffer before the sample was added and elution of the purified liposome fraction was collected based on turbidity, pooled together, and diluted to a final volume of 1.5 mL. This protocol for 1X liposome batch was used in all experiments below and the amount was adjusted to meet the need of the individual experiment by scaling up.

Dynamic Light Scattering Measurements: Dynamic Light scattering (DLS) measurements were carried out using a Malvern Zetasizer Nano S90 as quality control. Each liposome preparation was analyzed using DLS and only used when the size was +/− 50 nm from the intended and with a polydispersity below 0.25 unless other was stated.

Concentration Determination of EAR Stocks: The sulfhydryl concentration of the EAR in N-Methyl-2-pyrrolidone (NMP) stock was determined using a 5,5′-dithio-bis-(2-nitrobenzoic acid) (DTNB) standard curve of L-Cysteine (L-Cys).[23] The EAR stocks were diluted 100-fold upon addition to a 1 mM DTNB solution in a 0.1 mM sodium phosphate pH 8 buffer and left to react for 10 min before absorbance was measured at 412 nm using a plate reader. The concentration of free thiols in the EAR stocks was determined using the slope of the standard curve.

Incorporation of EAR into Liposomes: Liposomes were prepared as stated in the general liposome protocol. EAR was added to the liposomes in a 2X concentration from an *N*-Methyl-2-pyrrolidone (NMP) stock, as well as a control sample of liposomes with an equivalent percentage of NMP was prepared. The samples were incubated at RT for 30 min followed by the addition to a black 96-well plate where liposomes were diluted 1:1 resulting in a final concentration of EAR as 1X in each well. The final 1X EAR concentrations were stated in each independent experiment protocol.

General Procedure for Kinetic Experiments: Control samples received HEPES buffer to have an equivalent final volume (100 µL) and kinetic measurements of AMC were immediately monitored using a microplate reader at 37 °C for 2 h. The experiment was performed in three independent

biological replicates (with independent liposomal preparations) including two technical replicates for each sample. The data represent the mean ± SD.

Transmembrane Signaling in the Presence of External Maleimide Inhibitor: Liposomes were prepared as stated in the general liposome protocol, DLS was carried out as quality control and EAR was incorporated as stated above with a final concentration of 20 µM. In a black bottom 96-well plate samples with or without the external thiol-inhibitor methoxy-polyethylene glycol (5 kDa) maleimide (PEG-Mal) at a final conc. of 50 µM were prepared for all samples including 50 µL liposome sample with or without EAR and with or without 150 mg/L β-glucuronidase (GUS) was prepared. Samples receiving 10 µM DTT or 20 µM L-Cys were also included (identical thiol concentration). The above-described general procedure for kinetic experiments was performed.

Enzyme Selectivity in the Activation of Gus-EAR: Liposomes were prepared as stated in the general liposome protocol with EPC + 10 wt.% cholesterol, DLS was carried out as quality control and EAR was incorporated as stated above with a final concentration of 20 µM. In black bottom 96-well plate samples with 50 µM of the external thiol-inhibitor PEG-Mal, including 50 µL liposomes with or without EAR and with or without 150 mg L^{-1} GUS, β-glucosidase from almonds (GLU) or alkaline phosphatase (ALP) were prepared. A 10 µM DTT control with or without PEG-Mal was also included. The above-described general procedure for kinetic experiments was performed.

Investigating Lipid Composition: Liposomes were prepared as stated in the general liposome protocol with minor deviations in the lipid composition used for the formation of the film. The following five lipid compositions were used: "old" EPC (more than 6 months), EPC + 10 wt.% Cholesterol, EPC + 30 wt.% Cholesterol, 1-palmitoyl-2-oleoyl-glycero-3-phosphocholine (POPC), fresh EPC (new bottle). DLS was carried out as quality control and EAR was incorporated into all five liposome batches as stated above with a final concentration of 20 µM. In black bottom 96-well plate samples with or without 50 µM of the external thiol-inhibitor PEG-Mal, including 50 µL liposomes with or without EAR and with or without 150 mg L^{-1} GUS were prepared. Samples with either DTT or L-Cys in a final concentration of 10 and 20 µM were also included. The above-described general procedure for kinetic experiments was performed.

Dose Response of GUS: Liposomes were prepared as stated in the general liposome protocol with EPC + 10 wt.% cholesterol, DLS was carried out as quality control and EAR was incorporated as stated above with a final concentration of 20 µM. In black bottom 96-well plate samples with 50 µM of the external thiol-inhibitor PEG-Mal, including 50 µL liposomes with or without Gus-EAR and with GUS at a final concentration of 150, 15, or 1.5 mg L^{-1}. The above-described general procedure for kinetic experiments was performed. The represented data is normalized to the EAR + 150 mg L^{-1} GUS samples.

Effect of Liposomal Size: Liposomes were prepared as stated in the general liposome protocol with minor deviations in the liposome size, performed by differing the pore size of the used Whatman Nuclepore Track-Etched Membranes in the general liposome extrusion procedure. EPC liposomes were prepared using the pore size of 100, 200, 400, and 800 nm and DLS was carried out as quality control of the size and dispersity with a size that was +/− 70 nm from the intended and with a polydispersity below 0.3. EAR was incorporated as stated above with a final concentration of 20 µM for each independent liposomal batch. In black bottom 96-well plate samples with 50 µM of the external thiol-inhibitor PEG-Mal, including 50 µL liposomes with or without EAR and with or without 150 mg L^{-1} GUS were prepared. Samples with either DTT or L-Cys in a final concentration of 10 and 20 µM were also included. The above-described general procedure for kinetic experiments was performed. The represented data is normalized to the DTT control.

Visualization of Transmembrane Activation in Liposomes: Liposomes were prepared as described in the general protocol, with the only change that during hydration a 10X higher concentration of the fluorogenic substrate Arg-AMC (10 mM) was used. After preparation, the liposomes were equipped with Gus-EAR as stated in the general protocol at a final concentration of 500 µM. The liposomes were then purified through a NAP-25 column and samples with or without Gus-EAR were mixed with or without GUS (150 mg L^{-1}). The samples were incubated at 37 °C for 2 h and then analyzed using fluorescent microscopy. Image settings were adjusted on the +Gus-EAR+GUS sample and kept constant for all the other samples.

Preparation of GUVs: First, stocks of EPC, Cholesterol, mPEG-DSPE, and Liss-Rhodamine PE were dissolved in chloroform and diluted in mineral oil to a final concentration of 10 g L^{-1} for EPC, 5 g L^{-1} for Cholesterol, mPEG-DSPE; and 0.1 g L^{-1} for Rhodamine PE. The lipids were heated at 80 °C for at least an hour, and put overnight in a desiccator to evaporate all the chloroform.

A mixture containing 50 µL of pure mineral oil with 140 µL of EPC, 60 µL Cholesterol, 15 µL mPEG-DSPE and 25 µL Rhodamine PE from the stocks was prepared and heated for 2 min at 70 °C with shaking (800 rpm). Subsequently, the mixture was sonicated for 1 min, put back in the heating for 5 more minutes, and cooled down in ice for 15 min. After that time, the inner solution of the GUVs (25 mg L^{-1} papain, 4 µL BSA-FITC, 200 mM sucrose in Tris buffer (20 mM, 50 mM, NaCL, 30 mM MgCl, 10 mM spermidine, pH 7.9) was added on top of the lipid mixture and vortexed to emulsify the solution. When a milky white liquid was observed, it was put back in ice for 5 more minutes.

Finally, the mixture was added on top of the outer solution (200 mM glucose in Tris buffer) and centrifuged for 20 min at 5500 rpm. The oil (supernatant) was removed with a pipette until around 50 µL was left, including a white pellet in the bottom of the vial. 300 µL of outer solution were added to wash the pellet and the sample was centrifuged for 2 min at the same speed. This last washing step was repeated twice and a final volume of 50 µL of GUVs was collected.

Transmembrane Signaling in GUVs: In two 500 µL vials, 2.5 µL of GUVs in each were treated with 150 µM Gus-EAR (from a 21 mM stock in NMP) and completed to a final volume of 7 µL with outer solution. Another three vials were prepared as controls where the volume corresponding to Gus-EAR was replaced with the solvent NMP. Samples were incubated for 30 min, and then transferred to a see-through 96-well plate to a volume of outer solution to reach 50 µL total. Samples were treated with 100 µM DTT or 150 mg L^{-1} GUS. Microscope pictures were taken with an AxioCamMR3 camera after 45 min incubation at room temperature. Membrane lipids were visualized using a 43HE dsRED filter and green fluorescein from the substrate using 38 HE filter. Brightness and contrast were individually applied for each red channel, but for the green fluorescence (representing enzymatic activation) the same settings were applied. To obtain quantitative data, pixel intensity for the green channel was measured in all the GUVs (a total of 17 GUVs from two independent experiments) and plotted as bar graphs, as average fluorescent intensities representing enzymatic activation in each sample.

Supporting Information

Supporting Information is available from the Wiley Online Library or from the author.

Acknowledgements

A.B.S. and K.B.L. contributed equally to this work. The authors wish to acknowledge funding from the Independent Research Fund Denmark (DFF FNU Grant No 0135–00162B) and the Novo Nordisk Foundation (Grant No NNF20OC0062131).

Conflict of Interest

The authors declare no conflict of interest.

Data Availability Statement

The data that support the findings of this study are available from the corresponding author upon reasonable request.

Keywords

artificial receptors, chemical zymogen, synthetic cells, transmembrane signaling

Received: January 29, 2024
Revised: April 11, 2024
Published online: May 20, 2024

[1] a) R. Z. Moger-Reischer, J. I. Glass, K. S. Wise, L. Sun, D. M. C. Bittencourt, B. K. Lehmkuhl, D. R. Schoolmaster, M. Lynch, J. T. Lennon, *Nature* **2023**, *620*, 122; b) X. Qian, I. Nymann Westensee, E. Brodszkij, B. Städler, *WIREs Nanomed. Nanobiotechnol.* **2021**, *13*, e1683; c) M. A. Boyd, N. P. Kamat, *Trends Biotechnol.* **2021**, *39*, 927; d) B. C. Buddingh', J. C. M. van Hest, *Acc. Chem. Res.* **2017**, *50*, 769; e) E. Cho, Y. Lu, *ACS Synth. Biol.* **2020**, *9*, 2881.

[2] a) T. M. Chang, *Appl. Biochem. Biotechnol.* **1984**, *10*, 5; b) C. Xu, N. Martin, M. Li, S. Mann, *Nature* **2022**, *609*, 1029.

[3] M. P. Robertson, G. F. Joyce, *Cold Spring Harb. Perspect. Biol.* **2012**, *4*, a003608.

[4] a) L. Liu, Y. Zou, A. Bhattacharya, D. Zhang, S. Q. Lang, K. N. Houk, N. K. Devaraj, *Nat. Chem.* **2020**, *12*, 1029; b) A. Bhattacharya, L. Tanwar, A. Fracassi, R. J. Brea, M. Salvador-Castell, S. Khanal, S. K. Sinha, N. K. Devaraj, *J. Am. Chem. Soc.* **2023**,*145*, 27149.

[5] a) A. M. Wagner, H. Eto, A. Joseph, S. Kohyama, T. Haraszti, R. A. Zamora, M. Vorobii, M. I. Giannotti, P. Schwille, C. Rodriguez-Emmenegger, *Adv. Mater.* **2022**, *34*, 2202364; b) A. Belluati, S. Jimaja, R. J. Chadwick, C. Glynn, M. Chami, D. Happel, C. Guo, H. Kolmar, N. Bruns, *Nat. Chem.* **2024**, *16*, 564; c) N. Krinsky, M. Kaduri, A. Zinger, J. Shainsky-Roitman, M. Goldfeder, I. Benhar, D. Hershkovitz, A. Schroeder, *Adv. Healthcare Mater.* **2018**, *7*, e1701163; d) E. Brodszkij, I. N. Westensee, M. Bertelsen, N. Gal, T. Boesen, B. Städler, *Small* **2020**, *16*, 1906493.

[6] a) S. C. Shetty, N. Yandrapalli, K. Pinkwart, D. Krafft, T. Vidakovic-Koch, I. Ivanov, T. Robinson, *ACS. Nano* **2021**, *15*, 15656; b) B. Städler, R. Chandrawati, A. D. Price, S.-F. Chong, K. Breheney, A. Postma, L. A. Connal, A. N. Zelikin, F. Caruso, *Angew. Chem., Int. Ed.* **2009**, *48*, 4359.

[7] a) A. Armada-Moreira, B. Thingholm, K. Andreassen, A. M. Sebastião, S. H. Vaz, B. Städler, *Adv. Biosyst.* **2018**, *2*, 1700244; b) B. C. Buddingh', J. Elzinga, J. C. M. van Hest, *Nat. Commun.* **2020**, *11*, 1652.

[8] I. N. Westensee, E. Brodszkij, X. Qian, T. F. Marcelino, K. Lefkimmiatis, B. Städler, *Small* **2021**, *17*, 2007959.

[9] C. Zhu, F. Itel, R. Chandrawati, X. Han, B. Städler, *Biomacromolecules* **2018**, *19*, 4379.

[10] B. Yang, S. Li, W. Mu, Z. Wang, X. Han, *Small* **2023**, *19*, 2201305.

[11] R. Lentini, N. Y. Martín, M. Forlin, L. Belmonte, J. Fontana, M. Cornella, L. Martini, S. Tamburini, W. E. Bentley, O. Jousson, S. S. Mansy, *ACS Cent. Sci.* **2017**, *3*, 117.

[12] M. Dwidar, Y. Seike, S. Kobori, C. Whitaker, T. Matsuura, Y. Yokobayashi, *J. Am. Chem. Soc.* **2019**, *141*, 11103.

[13] T. Mashima, M. H. M. E. van Stevendaal, F. R. A. Cornelissens, A. F. Mason, B. J. H. M. Rosier, W. J. Altenburg, K. Oohora, S. Hirayama, T. Hayashi, J. C. M. van Hest, L. Brunsveld, *Angew. Chem., Int. Ed.* **2022**, *61*, e202115041.

[14] D. G. Andersen, A. B. Pedersen, M. H. Jørgensen, M. C. Montasell, A. B. Søgaard, G. Chen, A. Schroeder, G. R. Andersen, A. N. Zelikin, *Adv. Mater.* **2024**, *36*, 2309385.

[15] a) K. Bernitzki, M. Maue, T. Schrader, *Chem. - Eur. J.* **2012**, *18*, 13412; b) K. Bernitzki, T. Schrader, *Angew. Chem., Int. Ed.* **2009**, *48*, 8001; c) P. Barton, C. A. Hunter, T. J. Potter, S. J. Webb, N. H. Williams, *Angew. Chem., Int. Ed.* **2002**, *41*, 3878.

[16] a) M. J. Langton, F. Keymeulen, M. Ciaccia, N. H. Williams, C. A. Hunter, *Nat. Chem.* **2017**, *9*, 426; b) M. J. Langton, L. M. Scriven, N. H. Williams, C. A. Hunter, *J. Am. Chem. Soc.* **2017**, *139*, 15768.

[17] M. J. Langton, N. H. Williams, C. A. Hunter, *J. Am. Chem. Soc.* **2017**, *139*, 6461.

[18] J. Hou, J. Guo, T. Yan, S. Liu, M. Zang, L. Wang, J. Xu, Q. Luo, T. Wang, J. Liu, *Chem. Sci.* **2023**, *14*, 6039.

[19] L. Trevisan, I. Kocsis, C. A. Hunter, *Chem. Commun.* **2021**, *57*, 2196.

[20] a) H. Yang, S. Du, Z. Ye, X. Wang, Z. Yan, C. Lian, C. Bao, L. Zhu, *Chem. Sci.* **2022**, *13*, 2487; b) H. Li, Y. Yan, J. Chen, K. Shi, C. Song, Y. Ji, L. Jia, J. Li, Y. Qiao, Y. Lin, *Sci. Adv.* **2023**, *9*, eade5853.

[21] J. Hou, X. Jiang, F. Yang, L. Wang, T. Yan, S. Liu, J. Xu, C. Hou, Q. Luo, J. Liu, *Chem. Commun.* **2022**, *58*, 5725.

[22] C. Bravin, N. Duindam, C. A. Hunter, *Chem. Sci.* **2021**, *12*, 14059.

[23] A. B. Søgaard, A. B. Pedersen, K. B. Løvschall, P. Monge, J. H. Jakobsen, L. Džabbarova, L. F. Nielsen, S. Stevanovic, R. Walther, A. N. Zelikin, *Nat. Commun.* **2023**, *14*, 1646.

[24] a) M. Radzinski, T. Oppenheim, N. Metanis, D. Reichmann, *Biomolecules* **2021**, *11*, 469; b) M. S. B. Paget, M. J. Buttner, *Annu. Rev. Genet.* **2003**, *37*, 91; c) K. Ulrich, B. Schwappach, U. Jakob, *Biol. Chem.* **2021**, *402*, 239.

[25] a) M. C. Montasell, P. Monge, S. Carmali, L. M. Dias Loiola, D. G. Andersen, K. B. Løvschall, A. B. Søgaard, M. M. Kristensen, J. M. Pütz, A. N. Zelikin, *Nat. Commun.* **2022**, *13*, 4861; b) M. Casanovas Montasell, A. Baumann, A. N. Zelikin, *ChemBioChem* **2023**, *24*, 202300304.

[26] a) M. T. Jarlstad Olesen, R. Walther, P. P. Poier, F. Dagnæs-Hansen, A. N. Zelikin, *Angew. Chem., Int. Ed.* **2020**, *59*, 7390; b) P. Monge, K. B. Løvschall, A. B. Søgaard, R. Walther, T. W. Golbek, L. Schmüser, T. Weidner, A. N. Zelikin, *Adv. Sci.* **2021**, *8*, 2004432.

[27] R. Singh, W. A. Blättler, A. R. Collinson, *Anal. Biochem.* **1993**, *213*, 49.

[28] T. K. Harris, G. J. Turner, *IUBMB Life* **2002**, *53*, 85.

[29] G. A. R. Jamieson, D. M. Robinson, *Mammalian Cell Membranes*, Butterworth, London, **1977**.

[30] R. Walther, M. T. Jarlstad Olesen, A. N. Zelikin, *Org. Biomol. Chem.* **2019**, *17*, 6970.

